Journal of Thermal Analysis and Calorimetry, Vol. 90 (2007) 1, 299–306

EXPERIMENTAL INVESTIGATIONS FOR THE LOCATION OF REACTION ZONES IN A BAGASSE FIRED FURNACE

K. S. Shanmukharadhya[1*] *and K. G. Sudhakar*[2]

[1]Professor, Dept of Mechanical Engineering, Bannari Amman Institute of Technology, Sathyamangalam 638 401, India
[2]Principal and General Manager, Government Tool Room and Training Centre, Bangalore 560 044, India

It is unfortunately not too rare to find that fire investigators estimate flame temperatures by looking up a handbook value, which turns out to be the adiabatic flame temperature. Generally, the measurement of temperature in an industrial furnace is difficult, time consuming and expensive. Combustion of bagasse has its own special set of problems which appear to be due largely to the high moisture content and varying particle sizes of the fuel. The present experimental investigation is carried out to estimate the location of reaction zones and temperature fields in a bagasse fired furnace. Furnace is modeled by three dimensional CFD codes. Both experimental and the computational results show a considerable delay to ignition due to the drying of fuel. Also the location of maximum temperature zones and the pattern of flame propagation inside the furnace are clearly indicated.

Keywords: *bagasse, CFD, combustion, fuel moisture, reaction zones, temperature*

Introduction

Combustion instability in bagasse-fired furnaces is a key issue for operation but is presently not well understood. During periods of instability, there is considerable dulling of the flame, the furnace pressure oscillates, large mounds of wet fuel accumulate on the grate and it becomes impossible to maintain the mill steam requirements. Moisture is the 'single factor limiting the further development of bagasse suspension firing' [1]. In fact, one of the key motivations for this present research is the detrimental effect that the fuel moisture can have upon the boiler operation. In order to gain insight into the location of temperature fields and the reaction zones, experimental program was carried out on an operating, industrial size bagasse-fired furnace. Temperatures are recorded at key points of interest. The furnace was modeled by using three dimensional computational fluid dynamics package FLUENT by incorporating various submodels. The experimental data set provides a valuable base for the validation of the computational side of this present work. Both experiment and calculations clearly display the temperature zones and their distribution within the furnace.

Studies related to the behavior of bagasse combustion has revealed that the flame front is not attached to the bagasse spreaders and also a continuously burning bed at the rear of the furnace is desirable to stabilize the combustion. k–ε turbulence model have been used for bagasse combustion [2]. Finite volume approach for moeling bagasse combustion has been carried and time dependent equations for conservation of mass, momentum, energy and chemical species are solved [3]. The effect of fuel moisture has been investigated connected with the steady state calculations of a bagasse furnace and reported that the combustion activity reduces when the moisture level reaches 60% [4]. The effect of fuel moisture on pyrolysis and the effect of 'flash ignition' on wetter particles are carried by some researchers [5]. The intensity of combustion and energy efficiency will be affected by the moisture content of the fuel [6]. Some experimental investigations have reported that the heat conduction through the dry outer shell is a controlling factor in the drying of bagasse cylinders [7]. The steady state and time dependent calculations to investigate the instability in bagasse fired furnaces due to moisture of the fuel and various operating parameters have been well predicted in a bagasse fired furnace [8]. The influences of boiler operating parameters such as excess air and boiler load on emissions in a bagasse fired furnace have been studied and evaluated [9]. The deposition behaviour at various parts in the boiler is also investigated [10]. Excess air has a key operating variable and plays a vital role in achieving the higher combustion efficiency [11]. In the present work the temperatures are measured at various points in the furnace to locate the maximum temperature zones, pattern of flame propagation within the furnace. The DSC and TG-DTA for the bagasse are performed to study the thermal degra-

* Author for correspondence: kss_bit05@yahoo.co.in

1388–6150/$20.00

Akadémiai Kiadó, Budapest, Hungary
Springer, Dordrecht, The Netherlands

dation. The test furnace used for this work has tangential over fire air system to aid the combustion of bagasse in suspension and under grate air is the primary air. The operating characteristics, flow pattern, and the model of mixing in a furnace with tangential over fire air system has not been adequately investigated [12].

Furnace description

The furnace used for the test is a traveling grate spreader stoker furnace with tangential over fire air system to aid the suspension burning of the fuel. The two important input parameters are bagasse and air. The main source of air for combustion are under grate air (65% of the FD air), tangential over fire air (30% of the FD air) and distributor air (5% of the FD air). There are 5 air distributors placed below the bagasse spreaders. The test boiler operates at a nominal power of 20 MW. The bagasse spreaders (5 Nos) are spaced evenly in horizontal on the front wall of the furnace. The air coming from the tangential ducts forms a large vortex in the furnace. The size of the vortex depends on the tilt angles and dimensions of the furnace. These air flows from all the four ducts resulting in efficient mixing, due to vortex, rapid contact between fuel and air, and flame interaction, that would ensure a reliable combustion with uniform temperature distribution. Figure 1 shows the location and angle of tangential over fire air openings on the water wall.

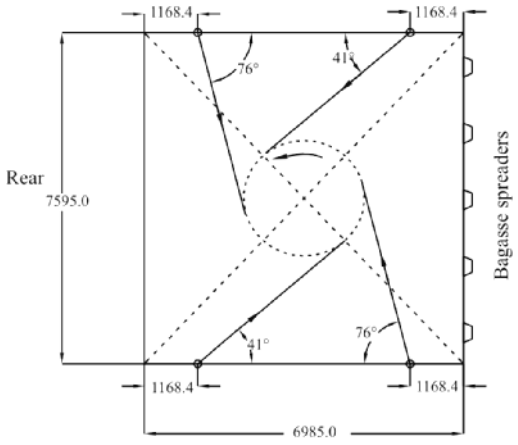

Fig. 1 Location and angle of tangential over fire air openings on the water wall

Experimental

In order to gain insight into the location of reaction zones and temperature distribution, an experimental program was carried out on the furnace. The measured bagasse input was 9.13 kg s^{-1}. The main sources of air for combustion are under grate air (26 kg s^{-1}), tangential over fire air (15 kg s^{-1}) and distributor air (2 kg s^{-1}). Also the velocity of under grate air (6 m s^{-1}), tangential duct air (23 m s^{-1}) and distributor air (36 m s^{-1}) are noted. The initial velocity of bagasse from the spreaders was assumed to be the same as the distributor air velocity. Since it is the air which carries the fuel into the furnace. Furnace wall temperature was 623 K and the moisture of the fuel was 51% during the measurements.

During the experiments made on the furnace, the boiler operating parameters were noted regularly during the test period. The percentage of moisture of the fuel was tested during the test period by using a MB45 moisture analyzer. A specially built *k*-type chromel–alumel thermocouple in a flexible 316 SS tubing (8 mm) was used to measure the temperature. A digital temperature indicator was used to record the temperature. Samples of bagasse were tested for thermogravimetric and differential thermal analysis by using an STA 1500 analyzer. Throughout the test period, the boiler was observed to run continuously not showing signs of gross instability while samples of bagasse had moisture contents as high as 54 and as low as 47%. All the flame temperature measurements were taken while the bagasse moisture content was within this range. When the boiler did experience problems, additional samples of bagasse were collected and tested at laboratory for the moisture level and found on the higher side. At these times there was a noticeable dulling of the light coming from the windows at the grate level and large mounds of bagasse could be seen to be piling up on the grate, in front of the spreaders. The mounds of bagasse at times were in excess of half to one meter in height. The operating conditions and properties of the fuel at 100% MCR (maximum capacity rating) are noted. The furnace was found operating with an equivalence air/fuel ratio of 4.3:1. While the calculated stoichiometric air/fuel ratio was 3.78:1.

The grate temperature was measured from both the front and rear grate openings. The measurements were made at all the seven grate openings. The various locations where temperatures were recorded on front and rear walls of the furnace are as shown in Fig. 2. The measurements were also made at several points at the level of tangential over fire windows, at a height of 3.8 m above the grate, at a height of 8.2 m above the grate on the rear wall and 10.17 m above the grate on front wall near the neck region of the furnace where maximum temperature was recorded.

Computational modeling

The furnace was modeled by using three dimensional computational fluid dynamics package FLUENT. The

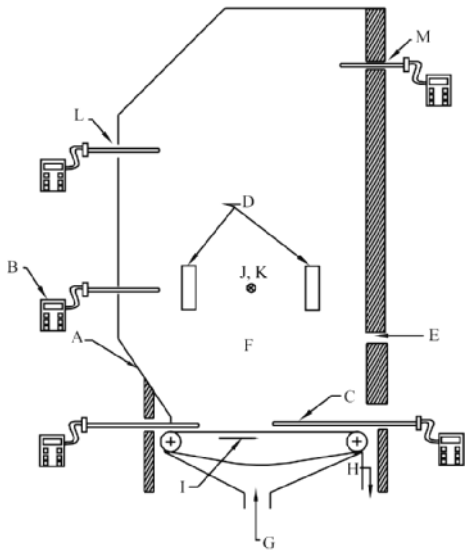

Fig. 2 System set up for the experimental measurements; A – sloping back of the furnace, B – digital indicator for temperature measurement, C – thermocouple, D – tangential over fire air windows, E – bagasse spreader, F – combustion chamber, G – undergrate air, H – to ash hopper, I – direction of travel of the grate, J and K – thermocouple positions on the side walls, L and M – thermocouple positions near the neck of the furnace

segregated implicit solver was used for solving the transport equations. The turbulence was modeled by standard k–ε model. Radiation is modeled by using P1 model. Species transport was used for combustion and combustible particles were assumed for bagasse particles. Devolatilization of bagasse is modeled by using Arrhenius kinetic mechanism [10].

$$\frac{d\eta}{dt} = k(\eta^* - \eta) \quad (1)$$

where η is the mass of volatiles released divided by the original dry sample mass, η* is the ultimate mass of volatiles released divided by the original dry sample mass. The ultimate mass of volatiles (η*) is determined as fraction of the original dry sample mass, including ash. Here k is the Arrhenius coefficient given by

$$k = A\exp\left(-\frac{E}{RT}\right) \quad (2)$$

The kinetic parameters [13] for sugarcane bagasse under conditions approximating the 'flash pyrolysis' experienced in the furnace. In Eq. (2), the pre-exponential A=2.13·10^6 s^{-1} and the activation energy E=101.3 kJ mol^{-1}. The ultimate yield for bagasse volatiles is 98.8% on a dry ash free basis. The values are global reaction values and follows first order reaction. The values are global reaction values and follows first order reaction. Char combustion is modeled using coal-char model [14], with char combustion kinetics [4].

Results and discussion

The computational model developed agrees qualitatively with the experimental data collected. The temperature measured on the grate had variation in the increasing order from the furnace front to the rear. The temperature found higher at the rear end of the furnace. Also measurements were made at the level of tangential ducts at the rear side of the furnace above the grate and found about 1380 K. The measurements made at the rear side of the furnace at a height of 8.2 m had temperature around 1460 K and the maximum temperature of about 1520 K measured at the level of the furnace neck at a height of 10.7 m above the grate. This maximum temperature zone later leads to the super heaters zone. Table 1 gives the temperatures measured at various points on the furnace connected with Fig. 2.

There are two main zones of intense combustion activity appears in the furnace. One is located on and above the sloping rear wall of the furnace. It is due to combustion of larger particles which are projected to the back of the furnace by the spreaders. Temperatures in excess of 1300 K arise in this region. Here the combustion activity predicted on the rear wall extends for the complete width of the furnace.

Figure 3 shows the measured and predicted values at the grate level. During measurements, temperatures were recorded along the grate depth at grate level. The trend in increasing temperature towards the back wall matches with the predicted temperature. It indicates the delay to ignition due to drying and heat up of the fuel. Also this high temperature at the rear of the furnace is due to combustion of larger particles which are projected to the back of the furnace by the spreaders.

A second combustion zone arises in the upper part of the furnace beyond the cool pre-ignition zone. This high temperature region is due to the ignition of lighter

Table 1 Measured and predicted temperatures at various points on the furnace

Measurements at the furnace center plane	Measured temperature/K	Predicted temperature/K
At 1 m in front of the grate (front wall)	712	746
At 3.86 m above the grate (rear side)	1381	1370
At 8.2 m above the grate (rear wall)	1468	1450
At 10.7 m above the grate (front wall)	1525	1520

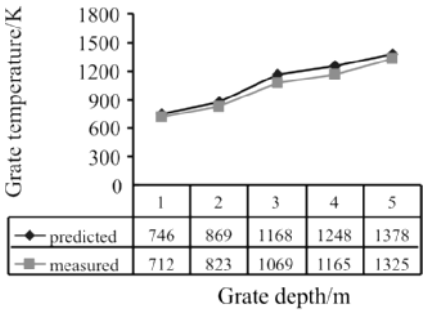

Fig. 3 Measured and predicted temperatures along the grate depth

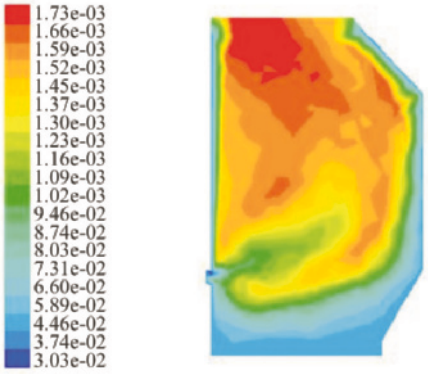

Fig. 4 Temperature in K at the centre spreader plane

bagasse particles that are swept upward by the vertical gas stream. Finally near the neck of the furnace the temperature raises to 1500 K. This is shown in Fig. 4.

The kinetics of the pyrolysis of sugar cane bagasse and other biomass materials has been the subject of much discussion. The result of the TG and DTA analysis carried out for the fuel are given in Figs 5 and 6. Two samples with moisture 49, 53% were tested. The moisture content of the bagasse coming out of the industry normally lies between 47–53%. Test samples are collected at different timings.

Figures 5 and 6 shows the mass loss (TG curve) and rate of mass loss (differential thermal analysis, DTA) with respect to temperature at the heating rate of 10°C min^{-1}. The curve was analyzed to obtain dry-

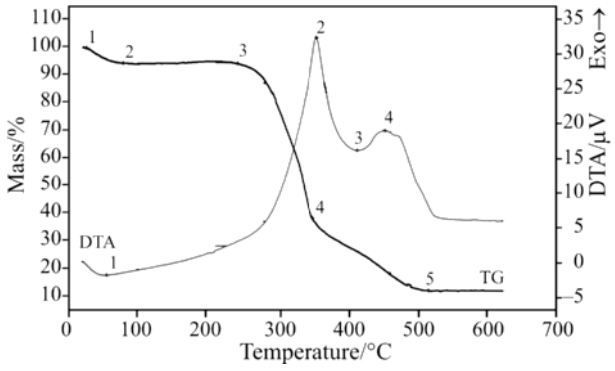

Fig. 5 TG and DTA analysis result for bagasse at moisture 49%

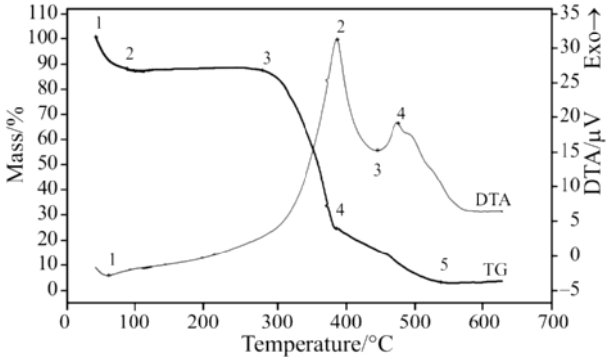

Fig. 6 TG and DTA analysis result for bagasse at moisture 53%

ing and pyrolysis characteristics, thermal degradation rates, initial and final temperatures of pyrolysis reaction zones and total degradation percent. The results of general drying and pyrolysis behavior and different zones during pyrolysis are given in Table 2. As seen from TG analysis three distinct zones or regions occur during the bagasse pyrolysis. The first zone is from the ambient temperature to onset of active pyrolysis. Initially, in this zone, the mass loss of the material occurs due to demoisturisation which starts around 25°C, peaks at 78°C with reference to Fig. 5. The total mass loss in this stage is 5–6% of the wet sample. Thereafter, the curve manifests an almost horizontal line with slight loss of mass which is followed by an onset of degradation of the material as evinced by first visible loss of mass after the horizontal line. Past workers [15–17] have found that this degradation in bagasse is either due to removal of bound form of moisture or due to evaporation of light volatile matter. The second zone represents the major decomposition of the material and is considered to occur between the initial temperature 241°C and the final temperature 350°C, obtained by the intersection of the adjacent straight line parts of TG curve and are considered as the active or first pyrolysis zone. This step manifests the intense loss of mass at rapid rates, and release of different types of volatiles. The third zone represents temperature above the final temperature of active pyrolysis zone 350°C and is also considered as passive pyrolysis or second pyrolysis zone. In this zone, the amount and rate of mass loss is lower and slower than the active pyrolysis zone. Previous work on bagasse, has reported that the cracking of C–C bonds occur between 350–516°C [17]. In this zone the carbon and ash content of the material increases [18]. The major degradation of bagasse occurs between 300 and 500°C and leads to rapid reduction of char yield between these temperatures [19]. The other line connected with differential thermal analysis indicates the peak temperatures at which the various stages of degradation proceeds. In Fig. 5, point 2 on DTA line corresponding to around 350°C and the maximum mass

Table 2 Drying and pyrolysis characteristics of bagasse at different moistures levels

Zone and characteristics		49%		53%	
Zones	pyrolysis characteristics	temperature range/°C	mass loss/%	temperature range/°C	mass loss/%
1–2	demoisturisation	<77.89	5.435	<65.46	13.843
2–3	thermally stable	77.89–241.15	0.028	65.46–251.18	2.262
3–4	active pyrolysis	241.15–349.51	55.272	251.18–355.19	55.805
4–5	passive pyrolysis	349.51–516.38	25.995	355.19–490.41	19.954
Beyond 5	thermally stable	>516.38	13.27 (ash)	>490.41	8.136 (ash)

loss in the third step occurs at 413°C. The two stages of pyrolyis are indicated by 1–2 and 2–3. 3–4 is char burning. It also implies that the thermal degradation of the sample in air up to 600°C is two-step degradation because the first step mass loss is due to moisture loss.

Previous research conducted on a variety of biomass including bagasse has shown that volatiles of different nature (both tar and non-tar) are released at following temperature ranges: less than 200, 200–280, 280–320 and 320–500°C [18, 20]. It is considered that the biomass is made up of various constituents, which decompose at different temperature regions. At temperature less than 100°C, biomass losses mainly moisture; between 100–250°C, extractives start decomposing; between 250 and 350°C predominantly hemicellulose decomposes; between 350 and 516°C cellulose and lignin decomposition occurs. At temperatures above 516°C, mainly lignin decomposes and contributes to char formation [15–18, 21].

Differential scanning calorimetry (DSC) is a thermoanalytical in which the difference in the amount of heat required to increase the temperature of a sample and reference are measured as a function of temperature. DSC is a thermal analysis method that measures the heat evolution from a sample under a controlled temperature scan and is under continuous development [22]. The raw bagasse and the larger particles selected from the raw bagasse are tested for DSC analysis by using Mettler Instrument. The larger particles were selected, because these are the particles causing problem during combustion due to heap formation. Due to their moisture content and size they get deposit in front of the spreaders and affects flame stability. In Fig. 7 the endothermic reaction reaches the peak around 50 mW, this is due to its moisture content. While the DSC results for larger particles shown in Fig. 8, the endothermic peak reaches around 23 mW. These particles are greater than 2057 micron in diameter and few centimeters in length. The difference is due to the raw bagasse consisting of particles with various sizes, which measures few centimeter in diameter and length, which consumes more heat before it starts degradation.

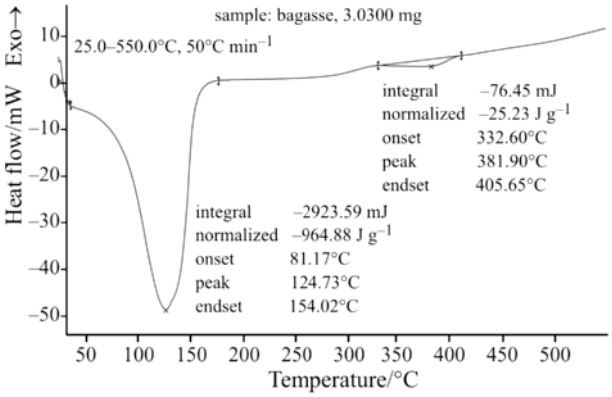

Fig. 7 DSC analysis of raw bagasse

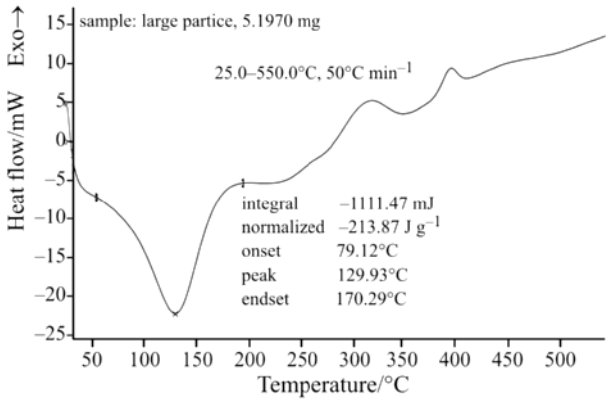

Fig. 8 DSC analysis of selected larger particles from the raw bagasse

Figure 9 shows the comparison of differential scanning calorimeter analysis results for the three samples. The particle with size 250 micron attains the endothermic peak at 90.64°C during which it consumes –6 mW. The particle with size 1003 micron reaches its peak temperature of 97.25°C and consumes around –7.5 mW. While it is around –23 mW for larger particles and around –50 mW for raw bagasse. This analysis clearly indicates that the particle sizes influences the heat absorption rate, which is a significant factor for combustion.

Figure 10 shows the effect of tangential air resulting in circular temperature distribution towards

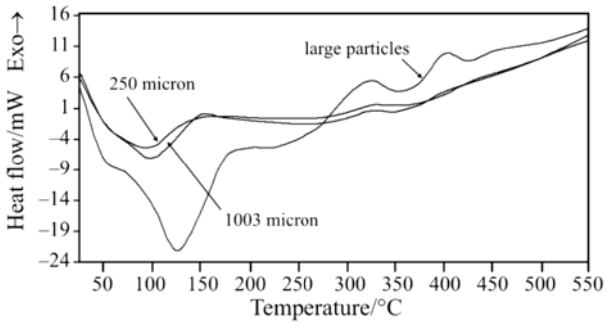

Fig. 9 DSC results for various sized bagasse particles

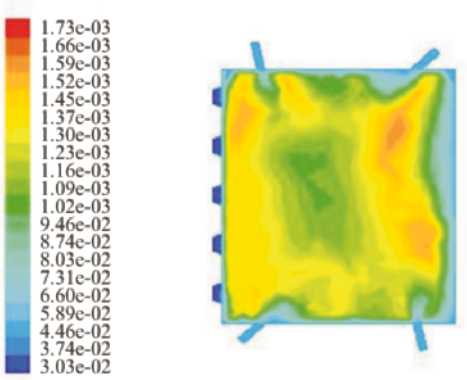

Fig. 10 Temperature distribution at the tangential over fire air windows level

the furnace wall. The air coming from the ducts forms a large vortex in the furnace resulting in efficient mixing of the fuel and air. Due to vortex, rapid contact between fuel and air, and flame interaction, that would ensure a reliable combustion with uniform temperature distribution.

Figure 11 shows the experimental and the predicted temperatures measured in front of all the grate openings at a distance of 1 m. The front end of the grate normally possesses the burnt ash which is traveling from the back and some unburnt particles which are heavy and fall in front of the grate. There will be bed of hot ash in this zone and extends for the whole width of the furnace.

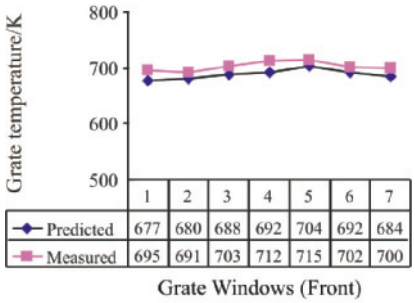

	1	2	3	4	5	6	7
Predicted	677	680	688	692	704	692	684
Measured	695	691	703	712	715	702	700

Fig. 11 Grate measurements from the front grate openings at a distance of 1 m

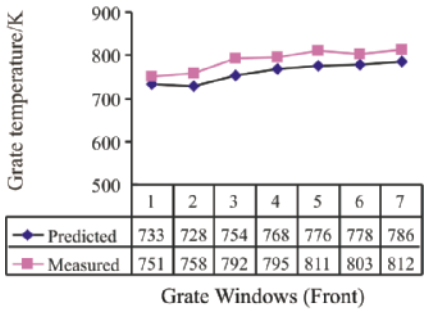

	1	2	3	4	5	6	7
Predicted	733	728	754	768	776	778	786
Measured	751	758	792	795	811	803	812

Fig. 12 Grate measurements from the front grate openings at a distance of 2 m

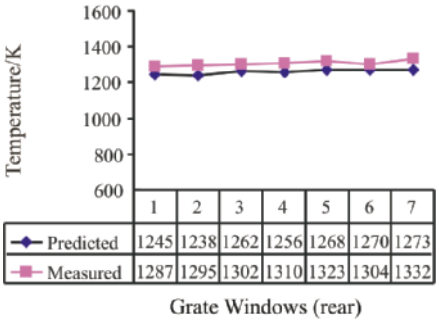

	1	2	3	4	5	6	7
Predicted	1245	1238	1262	1256	1268	1270	1273
Measured	1287	1295	1302	1310	1323	1304	1332

Fig. 13 Grate measurements from the rear grate openings at a distance of 1 m

Figure 12 shows the experimental and the predicted temperatures measured in front of all the grate openings at a distance of 2 m. Here the temperature across the width of the furnace higher than that measured at 1 m from the grate openings. This is due to the combustion of fuel particles on the grate.

Figure 13 shows the experimental and the predicted temperatures measured from the rear side of the grate openings at a distance of 1 m. The temperature is high in this zone due to the combustion of the particles which are coming down the sloping back where combustion takes place for most of the medium sized particles. Also the temperature distribution along the spreader plane clearly indicates that the combustion of bagasse takes place at the rear of the furnace.

A typical sample of bagasse encompasses a very wide range of particle sizes. Bagasse particles typically have dimensions of the order of 100 microns while the largest particles have maximum dimension of a few centimeters. The smallest particles follow the gas stream quite closely and are swept upwards after entry to the furnace, while the larger particles fall on to the grate. The smallest particle selected has a nominal diameter of 181 microns which is the diameter of an equivalent cylindrical particle.

The heat transfer takes place via both convection and radiation. The Spalding transport 'B' number approach is used to determine the mass transfer. The convection heat transfer coefficients are used in com-

puting the drying history of the particles. The 181 micron particle is dry after about 0.9 s, while the 668 micron particle, drying takes about 2 s. As the particle is projected further out into the furnace, its temperature increases and moisture mass loss progresses at a finite rate. From the particle size distributions it is apparent that the surface area to volume ratio of the 181 micron particle is around 4.6 times that of the 668 micron particle. Furthermore, the dry density of the larger particle is 4 times that of the smaller. The net result of this is that, per unit surface area, the 668 micron particle contains about seventeen times as much moisture as the 181 micron particle.

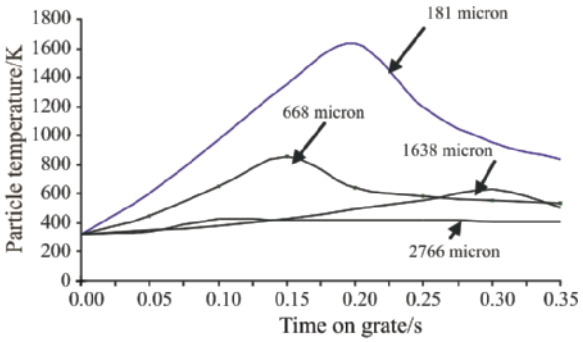

Fig. 14 Temperature profile of the particles

The temperature profile for particles 181, 668, 1638 and 2766 micron are shown in Fig. 14. The 181 micron particle reaches the maximum temperature around 0.2 s and reaches around 1630 K, while 668 micron particle reaches around 800 K, lesser than 181 micron particle due to its moisture content. The 1638 particle takes around 0.3 s to reach the maximum temperature during its travel along the grate and then it falls on to the grate. Similarly the 2766 micron particle reaches the maximum temperature around 0.1 s before falling on to the grate. The temperatures shown on the figure are combustion temperatures. The adiabatic temperature calculated was 1651 K. The temperatures attained by the particles are slightly less than the adiabatic temperature calculated. In the figure it is observed that as soon as the particle enters the furnace its temperature starts rising and the particle releases its volatile content then follows the thermal degradation. At the end of the curve it can be observed that due to some thermally stable minerals present in the fuel ash, the difference in temperature along the curve is negligible as the particle passes over the grate.

Figure 15 shows that the 181 micron particle reaches maximum velocity due to the influence of distributor air jet. Due to high velocity distribution air jet, the bagasse particles gain high velocity when it comes out of the spreader. The 181 micron particle reaches a

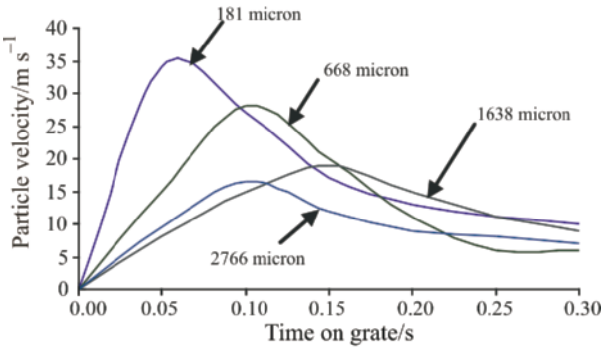

Fig. 15 Velocity of the particles on the grate

maximum velocity at around 0.02 s during which the particle gets dried and later it follows devolatilization and char burning. Similarly for 668 micron particle, due to its size and moisture content, it reaches its maximum velocity at around 0.2 s. Similarly the 1638 micron particle takes 0.14 s to reach the maximum velocity and it is about 0.1 s for the 2766 micron particle. The observation of the furnace justifies that the large clumps of fuel accumulation on the grate in front of the spreader to support the above.

Conclusions

The calculations and experiment clearly shows that much combustion activity occurs over the rear half of the test furnace. The fuel moisture does significantly affect the size of the pre-ignition zone and hence furnace stability. Fuel moisture plays a very important role in the initiation of instability in bagasse fired furnaces. Actual observations of furnace suggest that sudden changes in bagasse moisture which arise due to problems with mill operation appear to have a great effect on the furnace behaviour. Tangential air flow rates have an effect on the size of recirculation zone by forming an imaginary circle of flame inside the furnace to increase more heat transfer to the water walls. The analytical investigation made on the bagasse samples with different particle sizes also supports the simulation result made in this work. As the particle size increases, its tendency to absorb the energy increases during endothermic reaction with increase in time.

The maximum temperature attains at the neck of the temperature. It is found that raising the under-grate air flow can significantly increase the delay to ignition. Perhaps this may be attributed to the effect that the flow rate of under-grate air has upon the rate of deposition of fuel on the furnace grate. Also the bagasse and air flow rates through spreaders are found to have some influence on the ignition delay and the location on the furnace grate where the large particles come to rest.

Acknowledgements

The authors extend sincere thanks to the Management and workers of BAS Cogeneration plant Sathyamangalam for providing the necessary help during the experiments.

References

1 T. F. Dixon, Preliminary measurements in the flame region of a bagasse-fired boiler, Proceedings of Australian Society of Sugarcane Technologies, (1984), pp. 165–171.
2 B. E. Launder and D. B. Spalding, Computer Methods Appl. Mechanics Eng., 3 (1974) 269.
3 R. K. Boyd and J. H. Kent, Twenty-first Symposium (International) on Combustion, 21 (1986) 265.
4 M. Luo and B. R. Stanmore, J. Inst. Energy, 67 (1994) 128.
5 J. F. Stubington and S. Aiman, Energy Fuels, 8 (1994) 194.
6 T. Abbas, P. G. Costen and F. C. Lockwood, Twenty-sixth Symposium (International) on Combustion, 2 (1996) 3041.
7 P. Arici and B. R. Stanmore, Int. Sugar J., 99 (1997) 71.
8 P. Woodfield and J. Kent, Second International Conference on CFD in the Minerals and Process Industries, CSIRO, Melbourne, Australia 1999, pp. 299–304.
9 F. N. Teixeira and E. Silva Lora, Biomass Bioenergy, 26 (2004) 571.
10 S. Srikanth, S. K. Das, B. Ravikumar, D. S. Rao, K. Nandakumar and P. Vijayan, Biomass Bioenergy, 27 (2004) 375.
11 V. I. Kuprinov, K. Janvijitsakul and W. Permachart, Fuel, 85 (2006) 434.
12 F. El-Mahallawy and S. El-Din Habik, Fundamentals and Technology of Combustion, 1st Ed., Elsevier Energy Publishers, 2002.
13 A. F. Drummond, Ind. Eng. Chem. Res., 35 (1996) 1263.
14 I. W. Smith, Nineteenth Symposium (International) on Combustion, 19 (1982) 1045.
15 M. M. Nassar, E. A. Ashour and S. S. Wahid, J. Appl. Polym. Sci., 61 (1996) 885.
16 M. M. Nassar, Wood Fiber Sci., 17 (1985) 226.
17 P. Roque-Diaz, V. Z. Shemet and V. A. Lavrenko, Thermochim. Acta, 93 (1985) 349.
18 G. Várhegyi, M. J. Antal, T. Szekly and P. Szabó, Energy Fuels, 3 (1989) 329.
19 S. Katyal, K. Thambimuthu and M. Valix, Renewable Energy, 28 (2003) 713.
20 P. D. Grover, Thermochemical Characterization of Biomass, Vol. II, Indian Institute of Technology, New Delhi, India 1997.
21 M. A. Conners and C. M. Solazar, Proceedings Symposium on Forests Residues, International Achievements and Future, Vol. 5, Pretoria, S. Africa, 7–12 April 1985.
22 B. Wunderlich, J. Therm. Anal. Cal., 78 (2004) 7.

Received: May 29, 2006
Accepted: February 6, 2007
OnlineFirst: April 29, 2007

DOI: 10.1007/s10973-006-7703-2